

## Experimental Investigation of Heat Transfer and Friction Factor of V-shaped Rib Roughed Duct with and without Gap

Sachin Baraskar<sup>1</sup>. K.R.Aharwal<sup>2</sup>. A.Lanjewar<sup>3</sup>.

1. Assistant Professor Bhabha Engineering Research Institute
2. Associate Professor Maulana Azad National Institute of Technology,
3. Assistant Professor Maulana Azad National Institute of Technology,

### Abstract

Artificial roughness in the form of repeated ribs is generally used for enhancement of heat transfer from heated surface to the working fluid. This paper presents the experimental investigation of heat transfer and friction factor characteristics of a rectangular duct roughened with repeated v-shape ribs with and without gap on one broad wall arranged at an inclination of  $60^\circ$  with respect to the flow direction. A rectangular duct of aspect ratio of (W/H) of 8, relative roughness pitch (p/e) of 10, relative roughness height (e/D<sub>h</sub>) of 0.030, and angle of attack  $60^\circ$ . The heat transfer and friction characteristics of this roughened duct have been compared with those of the smooth duct under similar flow condition. The effect of gap in v-shaped rib has been investigated for the range of flow Reynolds numbers from 5000 to 14000. The maximum enhancement in Nusselt number and friction factor is observed to be 2.57 and 2.85 time of that of the smooth duct.

### Introduction

The thermal efficiency of solar air heaters has been found to be generally poor because of their inherently low heat transfer capability between the absorber plate and air flowing in the duct. In order to make the solar air heaters economically viable, their thermal efficiency needs to be improved by enhancing the heat transfer coefficient. In order to attain higher heat transfer coefficient, the laminar sub-layer formed in the vicinity of the absorber plate must be broken and the flow at the heat-transferring surface is made turbulent by introducing artificial roughness on the surface. However, the artificial roughness results in higher frictional losses leading to excessive power requirement for the fluid to flow through the duct. It is, therefore, desirable that turbulence must be created only in a region very close to the heat-transferring surface to break the viscous sub-layer for augmenting the heat transfer, and the core flow should not be unduly disturbed to limit the increase in friction losses. This can be done by keeping the height of the roughness elements small in comparison to the duct dimensions

Various investigators have studied different types of roughness geometries and their

arrangements to enhance the heat transfer from heat transferring surfaces. Han et al. [1] investigated the effect of angle of attack ( $\alpha$ ) and relative roughness pitch (p/e) on heat transfer and friction characteristics of rectangular duct with two roughened side walls. They reported that the maximum values of heat transfer coefficient and friction factor occur at relative roughness pitch of 10 at an angle of attack of  $45^\circ$  compared to the other rib arrangements under the requirements of same pumping power. Kiml et al. [2] reported that the rib roughness arrangement with an angle of attack of  $60^\circ$  shows better heat transfer performance compared to that of the  $45^\circ$  rib arrangement. Hu et al. [3] investigated the effect of inclined discrete rib with and without groove and reported that discrete rib arrangement without groove shows better thermal performance than that of the discrete rib with groove. Cho et al. [4] investigated the effect of a gap in the inclined rib on heat transfer in a square duct and reported that a gap in the inclined rib accelerates the flow and enhances the local turbulence which that will results in an increase in the heat transfer. They reported that the inclined rib arrangement with a downstream gap position shows higher enhancement in heat transfer compared to that without a gap i.e. of the continuous rib arrangement. Han et al. [5] reported that the rib configuration with relative roughness pitch of 7.5 gives higher enhancement in heat transfer than that of the relative roughness pitch of 10 or 5. Taslim et al. [6] investigated the heat transfer and friction factor characteristics of a channel roughened with angled and V-shaped ribs. They found that V-shaped ribs pointing downward have a much higher heat-transfer coefficient because the warm air being pumped toward the rib-leading region increases the apex region heat-transfer coefficients as compared to that of the leading end region. Han et al. [7] reported that  $45^\circ$  or  $60^\circ$  V-shaped ribs facing upward show higher heat transfer compared to corresponding V-shaped ribs facing downward. They found that V-shaped ribs facing upward forms two pairs of rotating cells along each divergent axis of rib, while in the case of V-shaped ribs facing downward, two pairs of counter-rotating cells merge resulting in a higher pressure drop and lower heat transfer. Han et al. [8] investigated the combined

effect of rib angle and channel aspect ratio. They reported that the maximum heat transfer and pressure drop is obtained at an angle of attack of  $60^{\circ}$  and a square channel provides a better heat-transfer performance than the rectangular channel. Cho et al. [9] examined the effect of angle of attack and number of discrete ribs, and reported that the gap region between the discrete ribs accelerates the flow, which increases the local heat-transfer coefficient. In a recent study, Lau et al. [10, 11] investigated the heat-transfer and friction factor characteristics of fully developed flow in a square duct with transverse and inclined discrete ribs. They reported that a five-piece discrete rib with  $90^{\circ}$  angle of attack shows 10–15% higher heat-transfer coefficient as compared to the  $90^{\circ}$  continuous ribs, whereas inclined discrete ribs give 10–20% higher heat transfer than that of the  $90^{\circ}$  discrete rib. Han et al. [12] carried out experiments to study the heat transfer and pressure drop characteristics of a roughened square channel with V-shaped broken rib arrangement with the angle of attack of  $45^{\circ}$  and  $60^{\circ}$  and reported that  $60^{\circ}$  V-shaped broken rib arrangement gives better performance than  $45^{\circ}$  V-shaped broken rib arrangement.

In view of the above, it can be stated that discrete inclined or V-shaped rib arrangement yields better performance as compared to continuous rib arrangement. However, investigations have not been carried out so far to see the effect of gap width between the rib elements to form the discrete rib. The present investigation was therefore taken up to see the effect of gap in v-shape rib to form a discrete rib. In the present work, experimental investigation on the performance of solar air heater ducts, having the absorber plate with artificial roughness in the form of v-shape rib with and without a gap, has been carried out. The flow Reynolds number has been varied between 3000 and 15,000. The variations of Nusselt number and friction factor as a function of roughness parameters including gap position have been evaluated to examine the thermo-hydraulic performance of the system to ascertain the benefit of this selected roughness geometry.

### **Experimental Setup**

The experimental schematic diagram set-up including the test section is shown in Fig.1. The flow system consists of an entry section, a test section, an exit section, a flow meter and a centrifugal blower. The duct is of size 2042mm x 200 mmX20mm (dimension of inner cross-section) and is constructed from wooden panels of 25 mm thickness. The test section is of length 1500mm ( $33.75 D_h$ ). The entry and exit lengths were 192 mm ( $7.2 D_h$ ) and 350 mm ( $12 D_h$ ), respectively. A short entrance length ( $L/D_h=7.2$ ) was chosen because for a roughened duct the thermally fully developed flow is established in a short length 2-3 hydraulic

diameter [14]. For the turbulent flow regime, ASHRAE standard 93-77 [14] recommends entry and exit length of  $5\sqrt{WH}$  and  $2.5\sqrt{WH}$ , respectively.

In the exit section after 116 mm, three equally spaced baffles are provided in an 87 mm length for the purpose of mixing the hot air coming out of solar air duct to obtain a uniform temperature of air (bulk mean temperature) at the outlet.

An electric heater having a size of 1500 mm x 216 mm was fabricated by combining series and parallel loops of heating wire Mica sheet of 1 mm is placed between the electric heater and absorber plate. This mica sheet acts as an insulator between the electric heater and absorber plate (GI plate). The heat flux may be varied from 0 to 1000  $W/m^2$  by a variac across it.

The outside of the entire set-up, from the inlet to the orifice plate, is insulated with 25 mm thick polystyrene foam having a thermal conductivity of 0.037 W/m- K. The heated plate is a 1 mm thick GI plate with integral rib-roughness formed on its rear side and this forms the top broad wall of the duct, while the bottom wall is formed by 1 mm aluminium plate and 25 mm wood with insulation below it. The top sides of the entry and exit sections of the duct are covered with smooth faced 8 mm thick plywood.

The mass flow rate of air is measured by means of a calibrated orifice meter connected with an inclined manometer, and the flow is controlled by the control valves provided in the lines. The orifice plate has been designed for the flow measurement in the pipe of inner diameter of 53 mm, as per the recommendation of Preobrazhensky [15]. The orifice plate is fitted between the flanges, so aligned that it remains concentric with the pipe.

The length of the circular GI pipe provided was based on pipe diameter  $d_1$ , which is a minimum of  $10 d_1$  on the upstream side and  $5 d_1$  on the downstream side of the orifice plate as recommended by Ehlinger [16].

In the present. experimental set-up we used 1000 mm ( $13 d_1$ ) pipe length on the upstream side and 700 mm ( $9 d_1$ ) on the downstream side. The calibrated copper- constantan 0.3 mm (24 SWG) thermocouples were used to measure the air and the heated plate temperatures at different locations. The location of thermocouples on the heated wall is shown in Fig. 1. A digital micro voltmeter is used to indicate the output of the thermocouples in  $^{\circ}C$ . The pressure drop across the test section was measured by a micro-manometer.

It is an open flow loop that consists of a test duct with entrance & exit sections, a blower, control valve, orifice plate and various devices for measurement of temperature & fluid head.

Parameter	Value
Reynolds Number (Re)	3000 – 15000
Roughness height (e)	1.4mm
Relative roughness height (e/ D <sub>h</sub> )	0.030
Relative roughness pitch (p/e)	10
Heat Flux (I)	800W/m <sup>2</sup>
Angle of attack	60 <sup>0</sup>
Channel Aspect ratio (W/H)	8
Test Length	1500mm
Hydraulic Diameter	44.44 mm

1. Air inlet section 2. Test section 3. Air outlet section 4. Varice 5. Selector switch 6. Mixing section 7. G.I. pipe 8. Orifice plate 9. Inclined U – Tube 10. Micro manometer 11. Flow control valve 12. Flexible pipe 13. Blower

**Fig. 1 Schematic Diagram Showing Top View of Experimental Setup**

**Roughness Geometry and Range of Parameters**

The values of system and operating parameters of this investigation are listed in Table 1. The relative roughness pitch (p/e) value is selected as 10, based on the optimum value of this parameter reported in the literature. Similarly, the value of the angle of attack is chosen as 60<sup>0</sup>, to achieve maximum enhancement of heat transfer. The arrangements of ribs on the absorber plate are shown in order to investigate the effect.

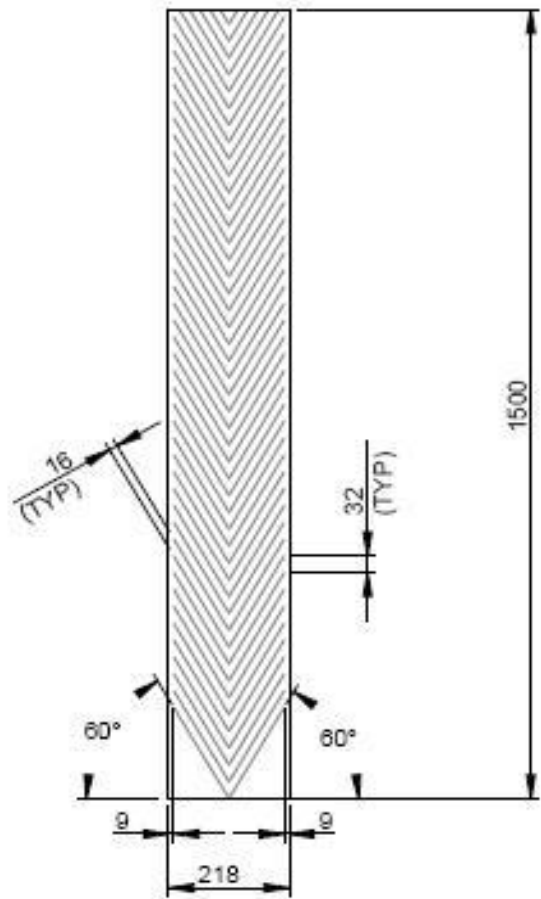
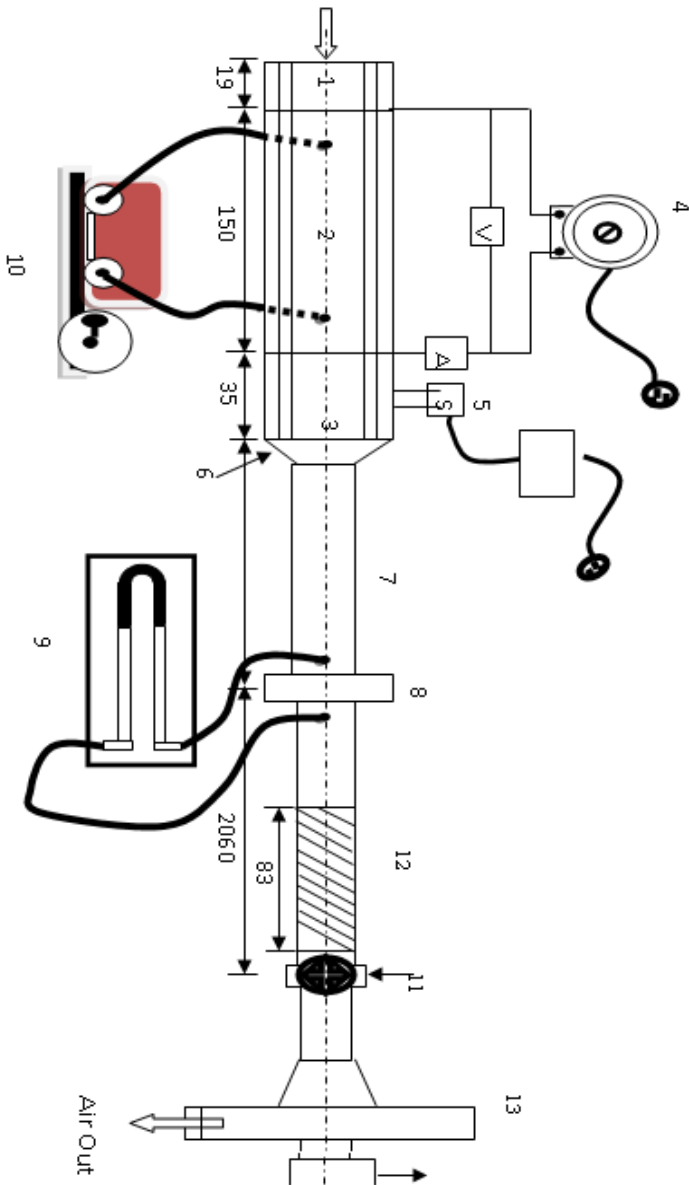


**Fig. 2 plate representing V-shape without gap**

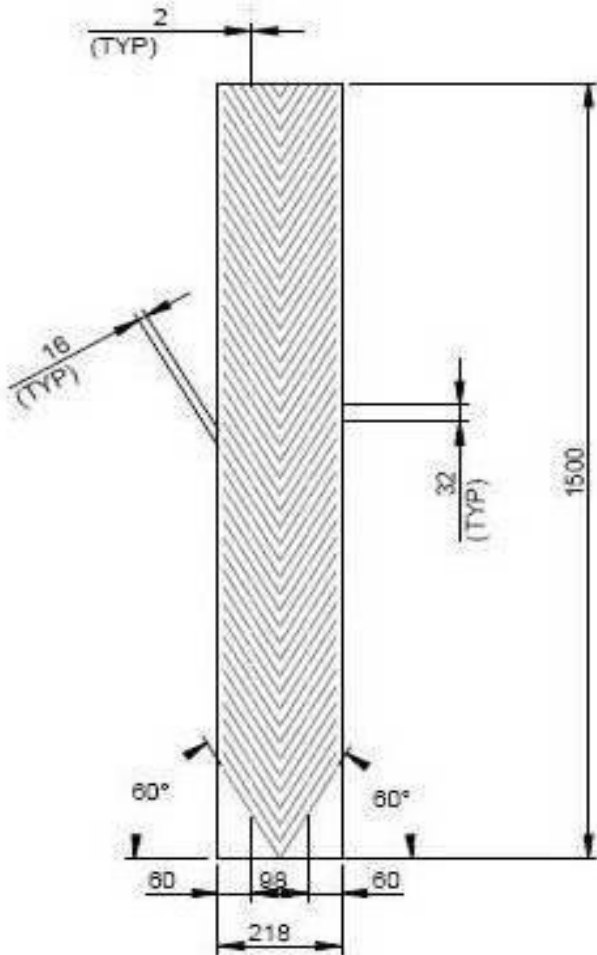


Fig. 3(a) plate representing V-shape with gap

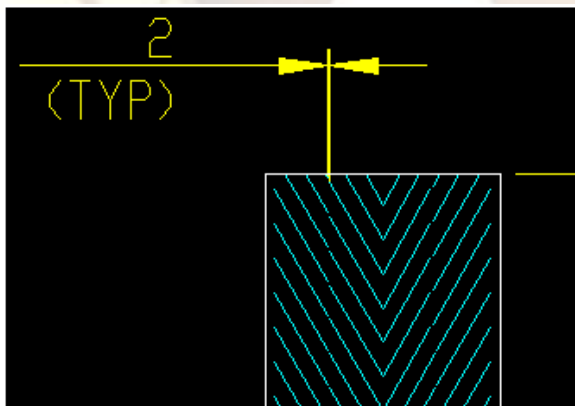


Fig. 3(b) Enlarge view of gap



Fig. 4 photo graphic view of absorber plate without gap



Fig.5 photo graphic view of absorber plate with gap

### Data Reduction

#### 1. Average Plate Temperature

Average plate data temperature is determined as follows:

$$T_{pav} = \frac{(Tp_1 + Tp_2 + Tp_3 + p_4 + Tp_5 + Tp_6)}{6}$$

#### 2. Average Outlet Air Temperature

Similarly the average air temperature is determined as :

$$T_{oav} =$$

#### 3. Pressure Drop Calculation

$$(T_{01} + T_{02} + T_{03} + T_{04}) / 4$$

Pressure drop measurement across the orifice plate by using the following relationship:

$$\Delta P_o = \Delta h \times 9.81 \times \rho_m$$

Where

- $P_o$  = Pressure diff. across orifice meter
- $\rho_m$  = Density of the manometer fluid
- $h$  = Difference of liquid head in U-tube manometer, m

#### 4. Mass Flow Measurement

Mass flow rate of air has been determined from pressure drop measurement across the orifice plate by using the following relationship:

$$m = C_d \times A_o \times [2 \rho \Delta P_o / (1 - \beta^4)]^{0.5}$$

Where -

- $m$  = Mass flow rate, kg / sec.
- $C_d$  = Coefficient of discharge of orifice i.e. 0.62
- $A_o$  = Area of orifice plate,  $m^2$
- = Density of air in  $Kg/m^3$
- = Ratio of orifice diameter to pipe diameter. ( $d_o / d_p$ ) i.e.  $26.5/53 = 0.5$

#### 5. Velocity Measurement:

$$V = m / \rho WH$$

Where -

- $m$  = Mass flow rate, kg / sec
- = Density of air in  $Kg/m^3$
- $H$  = Height of the duct in m
- $W$  = Width of the duct, m

#### 6. Reynolds Number

The Reynolds number for flow of air in the duct is calculated from:

$$R_e = VD / \nu$$

Where -

- □ = Kinematics viscosity of air at average fluid temperature

$$D_h = 4WH / 2 (W+H)$$

#### 7. Heat Transfer Coefficient

Heat transfer rate,  $Q_a$  to the air is given by:

$$Q_a = m c_p (t_o - t_i)$$

The heat transfer coefficient for the heated

test section has been calculated from:

$$h = Q_a / A_p (T_{pav} - T_{fav})$$

$A_p$  is the heat transfer area assumed to be the corresponding smooth plate area.

#### 8. Nusselt Number

Heat Transfer Coefficient has been used to determine the Nusselt number defined as;

$$\text{Nusselt No. (Nu)} = h D_h / K$$

Where  $k$  is the thermal conductivity of the air at the mean air temperature and  $D_h$  is the hydraulic diameter based on entire wetted perimeter.

#### 9. Friction Factor

The friction factor was determined from the flow velocity ' $V$ ' and the head loss ' $\Delta h_d$ ' measured across the test section length of 1m using the Darcy-Weisbach equation as

$$F = 2[(\Delta P)_d] D_h / 4\rho l v^2$$

#### 10. Thermo Hydraulic Performance

Thermo hydraulic performance is calculated by

$$T_{hp} = (N_u / N_{us}) / (f_r / f_s)^{1/3}$$

#### Validation of Experimental Set-up

In order to validate the experimental set-up, experiment have been performed by keeping all the surfaces of the duct smooth and the results of smooth duct wall compared with those of the theoretical results Fig. 6 shows the variation of nusselt number as a function of Reynolds number for smooth duct. It is observe that the deviation in the experimental results with theoretical is small. This show good agreement between theoretical & experimental results. similar results have been observed for the friction factor as shown in Fig. 7 which again shows the good agreement between experimental and theoretical results.

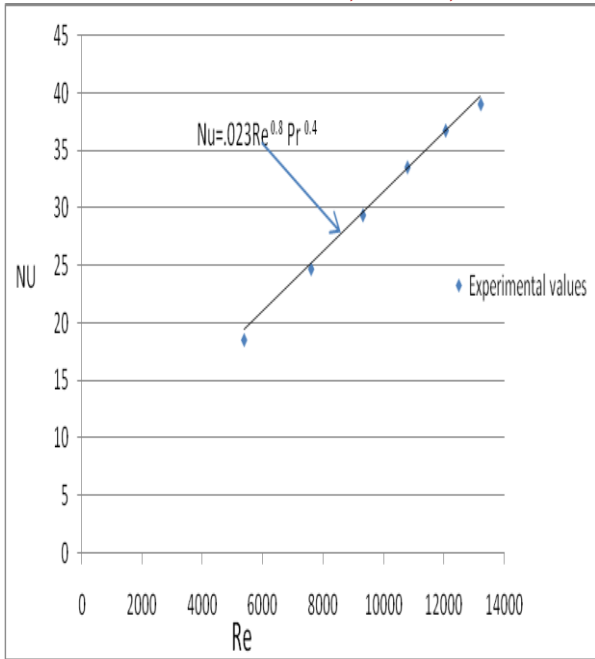


**Fig 6. Shows The Variation of Nusselt Number with Reynolds Number**

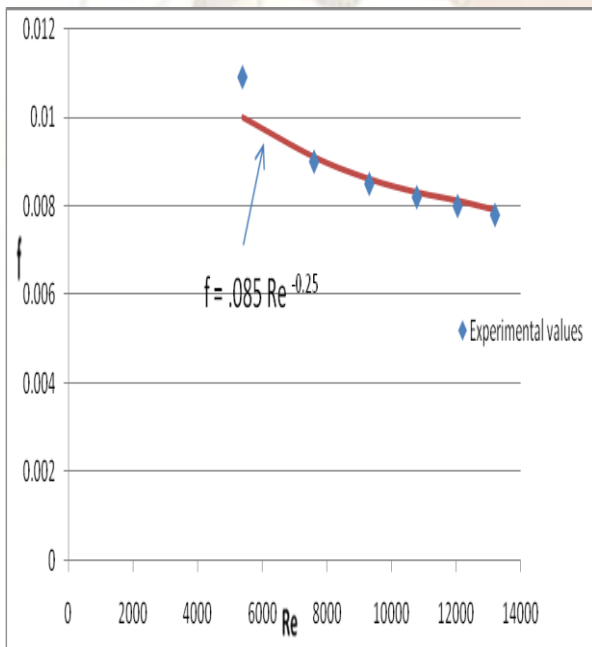


**Fig 7. Shows The Variation of Friction Factor with Reynolds Number**

**Results and Discussion**

Following results have been obtained from the experiment. The variation of Nusselt number with Reynolds number is shown in Fig. 8 It is seen that the value of Nusselt number increases with increases in Reynolds number. The value of Nusselt number is varies from 20 to 80 in the range of Reynolds number 5000-14000. The maximum value of Nusselt number is observe for rib with gap roughness arrangement. This may due to the fact that the presence of gap produce more turbulence,

which enhances the heat transfer.

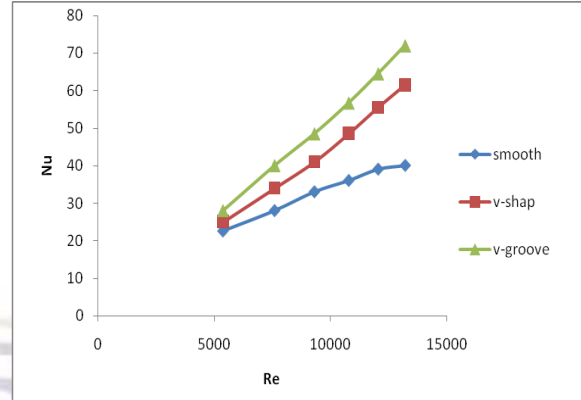


**Fig 8 Variation of Nusselt Number with Reynolds Numbers**

The variation of friction factor with Reynold number is shown in fig 9. It is seen that the value of friction factor decreases with increas in Reynold number. This may be due to the fact that as the Renold number increases, the thickness of boundary layer decreases therefore, friction factor decreases with increase in Reynold number. The maximum value of friction factor is observed for v-shaped rib with gap roughness arrangement, whereas it's minimum value is observed for smooth duct. The value of friction factor of v-shaped rib roughness arrangement is lower than that of the v-shaped rib with gap.

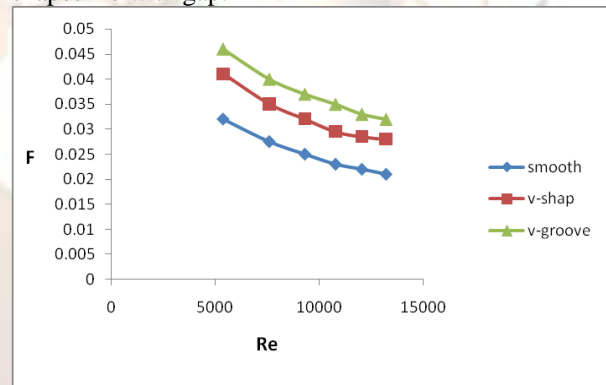


**Fig 9 Variation of Friction Factor with Reynolds Numbers**

The variation of thermo hydraulic performance with Renold number is shown in fig 10. It is seen that the value of Reynold number increases with increas in thermo hydraulic performance and after attaining maximum value, thermo hydraulic performance decreases with increase in Reynold number. The value of thermo hydraulic performance varies from 0.4 to 1.6 in the range of Reynolds number 5000-14000. The maximum value of thermo hydraulic performance obseved for v-shape with gap and minimum value is achieved for smooth plate.

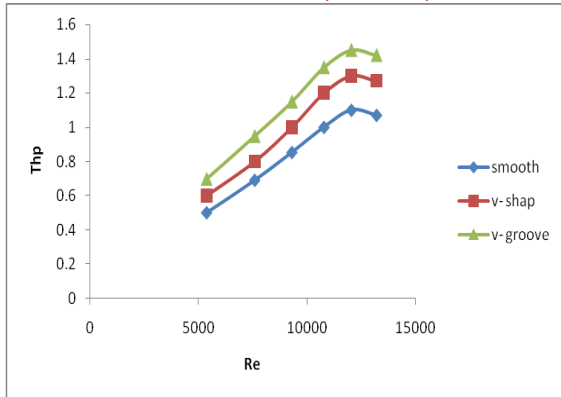


**Fig 10 Variation of Thermo Hydraulic Performance with Reynolds Numbers**  
**Conclusion**

The present work was undertaken with the objectives of extensive investigation into v shaped ribs as artificial roughness with and without gap on the on broad wall of solar air heater. Experimental setup for heat transfer and friction factor have been design and developed. Data were collected for heat transfer and friction factor of these artificially roughened duct. Results of artificially roughened duct have been compared with those of a smooth duct under similar flow condition to determine heat transfer and friction factor. The major conclusion draw from this investigation are given below-

Reynolds Number (Re)	3000 – 15000
Roughness height (e)	1.4mm
Relative roughness height (e/ D <sub>h</sub> )	0.030
Relative roughness pitch (p/e)	10
Heat Flux (I)	800W/m <sup>2</sup>
Angle of attack	60 <sup>0</sup>
Channel Aspect ratio (W/H)	8
Test Length	1500mm
Hydraulic Diameter	44.44 mm

- 1 The value of Nusselt number increases with increase in Reynold number. The maximum value of Nusselt number is observe for v-shape rib with gap roughness arrangement because the presence of v-shape with gap increases the level of turbulence, which cause enhancement in heat transfer.
- 2 The value of friction factor decreases with increase in the value of Reynold number. The maximum value of friction factor is observe for v-shaped with gap rib roughness arrangement. The value of

friction factor of v-shaped rib roughness arrangement is less than that of the v-shaped with gap.

- 3 It is observe that the value of thermo hydraulic performance parameter increases with increase in Reynold number the maximum value of this parameter is observe for v-shaped rib with gap roughness arrangements.

#### Nomenclature

A	Absorber plate area, m <sup>2</sup>
A <sub>duct</sub>	Flow Cross-section area = WH, m <sup>2</sup>
A <sub>o</sub>	Throat area of orifice plate, m <sup>2</sup>
A <sub>p</sub>	Area of absorber plate, m <sup>2</sup>
A <sub>s</sub>	Area of smooth plate, m <sup>2</sup>
C <sub>d</sub>	Coefficient of discharge (0.62)
C <sub>p</sub>	Heat of air at constant pressure,
D <sub>h</sub>	Equivalent diameter of air passage,
D <sub>o</sub>	Diameter of orifice plate, m
D <sub>p</sub>	Inside diameter of pipe, m
e	Roughness height, mm
e/ D <sub>h</sub>	Relative roughness height
f	Friction factor Δ
h	Convective heat transfer coefficient,
Δh	Difference of height on Manometer fluid
I	Heat Flux, W / m <sup>2</sup>
k	Thermal conductivity of air, W/m- °c
m	Mass flow rate of air, kg/s
Nu	Nusselt number
p	Pitch
p/e	Relative roughness pitch
ΔP <sub>o</sub>	Pressure drop across orifice meter,
Q <sub>a</sub>	Rate of heat transfer to air, W
Re	Reynolds number
T <sub>a</sub>	Atmospheric temperature, °c
T <sub>fav</sub>	Average temperature of air, °c
T <sub>i</sub>	Inlet temperature of air, °c
T <sub>o</sub>	Outlet temperature of air, °c
T <sub>pav</sub>	Average plate temperature, °c
V	Velocity of air, m/s
W/H	Channel aspect ratio

#### Greek Symbols

β	Ratio of orifice diameter to pipe diameter
η <sub>th</sub>	Thermal efficiency
ρ	Density of air, kg/m <sup>3</sup>
ρ <sub>m</sub>	Density of manometer fluid, Kg/m <sup>3</sup>
μ	Dynamic Viscosity, Kg/m-sec
ν	Kinematic Viscosity, m <sup>2</sup> / sec

#### References

1. Han J. C. "Heat transfer and friction in channels with two opposite rib roughened walls", Trans. ASME Journal of Heat Transfer, 106, 774-781, 1984
2. Kiml R. Mochizuki S. and Murata A. "Effects of rib arrangements on heat transfer and flow behavior in a rectangular

- rib roughened passage". International Journal of Heat and mass transfer; 123: 675-681, 2001
3. Hu Z. and Shen J. Heat transfer enhancement in a converging passage with discrete ribs. Int. Journal Heat and Mass Transfer 1996; 39 (8): 1719-1727
  4. Cho H.H, Kim Y.Y, Rhee D.H, Lee S.Y and Wu S.J. The effect of gap position in discrete ribs on local heat/ mass transfer in a square duct Journal of Enhanced heat transfer 2003; 10(3): 287-300.
  5. Han J.C., Glicksman LR and Rosenow WM. Investigation of heat transfer and friction for ribroughened surfaces, Int. Journal of Heat & Mass Transfer 1978; 21: 1143-1156.
  6. Taslin ME, Li T, Rercher DM. Experimental heat transfer and friction in channels roughened with angled, V-shaped and discrete ribs on two opposite walls. J Turbomachinery 1996;118:20-8.
  7. Han JC, Zhang YM, Lee CP. Augmented heat transfer in square channels with parallel, crossed, and V-shaped angled ribs. Trans ASME, J Heat Transfer 1991;113:590-6.
  8. Han JC, Park JS. Developing heat transfer in rectangular channels with rib turbulators. Int J Heat Mass Transfer 1988;3(1):183-95.
  9. Cho HH, Wu SJ, Kwon HJ. Local heat/mass transfer measurement in a rectangular duct with discrete ribs. J Turbomachinery 2000;122:579-86.
  10. Lau SC, McMillin RD, Han JC. Turbulent heat transfer and friction in a square channel with discrete rib turbulators. Trans ASME, J Turbo Machinery 1991;113:360-6.
  11. Lau SC, McMillin RD, Han JC. Heat transfer characteristics of turbulent flow in a square channel with angled rib. Trans ASME, J Turbomachinery 1991;113:367-74.
  12. Han JC, Zhang YM. High performance heat transfers ducts with parallel broken and V- shaped broken ribs. Int J Heat Mass Transfer 1992;35(2):513-23.
  13. Sukhatme S.P., "Solar Energy: Principles of Thermal Collections and Storage", Tata McGraw-Hill, New Delhi 1994.
  14. ASHARE Standard 93-97. Method of testing to determine the thermal performance of solar collectors, 1977.
  15. Preobrazhensky VP. Measurement and Instrumentation in Heat Engineering [English translation], vol. 2. Moscow: Mir Publisher, 1980.
  16. Ehlinger AH. Flow of air and gases. In: Salisbury JK, editor. Kent's Mechanical Engineers Hand- book, Power Volume. New York: Wiley, 1950:1.101.21.
  17. Prasad, K., and Mullick, S.C., 1985, "Heat transfer Characteristics of a Solar Air Heater Used for Drying Purposes", J. Applied Energy, Vol 13, pp. 55-64
  18. Karwa, R., Solanki, S.C., Saini, J.S., 2001, "Thermohydraulic Performance of Solar Air Heater having Integral Chamfered Rib Roughness on Absorber Plates", Int. J. Energy, Vol 26, pp. 161-176.
  19. Jain, A., Bhagoria, J.L., Sharma, M.C., 2005, "Thermal Performance of Solar Air Heater By Using Shot Peened Absorber Plate", Proceedings of 9<sup>th</sup> International Conference on Shot Peening, Paris, pp. 67-74.
  20. K.R. Aharwal, B.K. Gandhi, J.S. Saini "Experimental investigation on heat-transfer enhancement due to a gap in an inclined continuous rib arrangement in a rectangular duct of solar air heater", Renewable Energy, Volume 33, Issue 4, Pages 585-596, April 2008.
  21. S.V. Karmare, A.N. Tikekar, " Heat transfer and friction factor correlation for artificially roughened duct with metal grit ribs" International Journal of Heat and Mass Transfer, Volume 50, Issues 21-22, Pages 4342-4351, 2007.